Physical Communication 34 (2019) 105–113

Contents lists available at ScienceDirect

Physical Communication

journal homepage: www.elsevier.com/locate/phycom

Full length article

Cooperative AF relaying with energy harvesting in Nakagami-*m* fading channel

Mohammadreza Babaei [a], Ümit Aygölü [a], Ertugrul Basar [b,*]

[a] Electronics and Communication Engineering Department, Istanbul Technical University, 34469, Istanbul, Turkey
[b] Communications Research and Innovation Laboratory (CoreLab), Department of Electrical and Electronics Engineering, Koç University, 34450, Istanbul, Turkey

ARTICLE INFO

Article history:
Received 4 July 2018
Received in revised form 5 January 2019
Accepted 1 March 2019
Available online 12 March 2019

Keywords:
Energy harvesting
Cooperative AF relaying
Bit error probability

ABSTRACT

In this paper, the bit error performance of an energy harvesting (EH) cooperative amplify-and-forward (AF) relaying system, in which the relay harvests energy from radio frequency source signal and then uses this energy to transmit its signal to the destination in the presence of a direct link between the source and the destination, is investigated in Nakagami- *m* fading channel. A unified approach to the analysis of bit error probability (BEP) is presented for the cases where the relay harvests energy based on power splitting (PS), time switching (TS) and ideal operational modes. Simulation results validate the theoretical analysis performed for coherent *M*-PSK and *M*-QAM and different system parameters. Dual-hop EH and conventional non-EH cooperative AF relaying systems are considered for comparison purposes. The obtained results show that the system bit error rate performance is mostly dependent on the channel parameter *m* and the energy harvesting parameters.

1. Introduction

Recently, relaying techniques by energy harvesting (EH) have been considered as an interesting area of research to prolong the life time of mobile nodes and improve the system energy-efficiency. EH systems, in which the nodes extract energy from the received radio frequency (RF) signal [1–3], introduce self-sustainability to the power constraint devices. Early studies on the EH systems, introduce power splitting (PS), time switching (TS) and ideal (practically unrealistic) operational modes for power constraint nodes to harvest energy [2,3]. In PS mode, a portion of the incoming signal power is used for EH and the remainder for information processing (IP). In TS mode, a fraction of the signaling interval is used for EH and the remainder for IP. Finally, the ideal mode is similar to PS mode where the relay processes information and harvests energy from the total power of the incoming RF signal.

1.1. Prior related works

In [3–6], the outage analysis of dual-hop (DH) systems is performed, where the source and the destination only communicates via a power constraint relay when the link between the source and the destination is in deep fade. In [3], outage and ergodic capacities of a DH-EH system, where amplify-and-forward (AF) relay applies PS, TS and ideal operational modes, are presented. Analytical expressions for outage and ergodic capacities are obtained in Rayleigh fading channel, which are then used to derive throughput expressions. In [4–6], the outage performance of a decode-and-forward (DF) DH system is studied. In [4], ergodic capacity and throughput of EH system are derived for indoor channels characterized by log-normal fading while in [5], Rayleigh fading is considered. The reference [6] considers the case where, the relay harvests energy from both the source signal and the co-channel interference signals and then uses that energy to forward the correctly decoded source signal to the destination. In [6], channels are assumed to be exposed to Rayleigh fading and both delay-limited and delay-tolerant capacities are considered to obtain the analytical throughput expressions. Throughput of a multiple-input multiple-output DH system where the source communicates with the destination via an EH relay over a Nakagami-*m* fading channel is studied in [7], and both PS and TS EH modes are considered. In [8], for an DH-EH-AF relaying system, the outage and ergodic capacities are obtained and an adaptive receiver structure is introduced.

In [9–11], the performance of two-way (TW) EH relaying systems is investigated. In [9], a TW-AF EH system is studied where the power allocation problem is solved to maximize the energy efficiency under some system parameter constraints. Theoretical analysis is performed for PS EH mode under Rayleigh fading. In [10], a TW-AF relaying network, in which relay applies TS

* Corresponding author.
E-mail addresses: babaei@itu.edu.tr (M. Babaei), aygolu@itu.edu.tr (Ü. Aygölü), ebasar@ku.edu.tr (E. Basar).

https://doi.org/10.1016/j.phycom.2019.03.001
1874-4907/

EH mode to harvest RF energy coming from both sources, is analyzed. In [11], the outage probability and ergodic capacity of TW-AF relaying system are studied when links between nodes are exposed to Nakagami-m fading. TS mode is considered in [11] where the two sources are equipped with multiple antennas and the relay is equipped with only one antenna.

As an application of EH to cooperative relaying systems, in which a direct link is available between the source and the destination, the outage performance optimization for Rayleigh fading channels is provided in [12]. In [13], PS operational mode and antenna selection are jointly applied to a multiple-antenna power-constraint relay in an AF system to maximize the achievable rate.

In all of these studies, the outage analysis is preferred to evaluate the performance of the considered EH systems. Different from these works, in [14–16], the bit error performance of the system with an EH relay, is studied. In [14], the mixture of modulations approach for TS harvesting mode is introduced to maintain the spectral efficiency at a fixed value for all values of the TS mode parameter α. The system bit error probability (BEP) performance is obtained for an AF relay. In [15], a non-coherent multi-hop EH system is investigated, in which the relays forwards the signal to the next node. Furthermore, symbol error probability (SEP) is obtained for PS, TS modes and theoretical SEP results supports M-ary non-coherent frequency-shift keying (FSK) and differential phase-shift keying (DPSK) modulations. The BEP of DH-EH system for both AF and DF relaying is investigated in [16] for PS, TS and ideal operational modes, in which it is assumed that all links are exposed to Nakagami-m fading channel.

When multiple antennas are employed at all nodes, the harvested energy at relay and the received SNR at both relay and destination will be increased. Namely, more power will be harvested from S at R, which results as a more transmit power at the relay and subsequently more received SNR for the link R→D. Moreover, multiple antennas at the destination will also increase the received SNR for the link R→D. As a result, the BER performance of the whole system will be significantly increased. However, the case of multiple antennas is beyond the scope of this paper and can be considered as a future work.

1.2. Motivation and contribution

The majority of the works on EH systems have dealt with the outage performance [3–13], while only a small number of papers have studied the bit error rate (BER) performance as in [14,15], where except [16], Rayleigh fading is considered in aforementioned cases. To the best of our knowledge, the performance of EH cooperative AF relaying system for a coherent modulation subject to Nakagami-m fading has not been investigated yet. Motivated by this, we propose a unified BEP analysis for the EH cooperative AF system using the coherent M-PSK and M-QAM in Nakagami-m fading channels. The main contributions of this paper are summarized as follows.

- The analytical BEP of a three-node (source–relay–destination) cooperative relaying network, where an AF relay harvests energy from the RF source signal, is obtained.
- A unified cumulative distribution function (CDF) of signal-to-noise ratio (SNR) at the destination is derived and then used to obtain the closed-form BEP expression for PS, TS and ideal EH operational modes and further used to provide the performance results for both M-PSK and M-QAM schemes.
- The results are provided for a fixed spectral efficiency value of $R = 1$ bits/s/Hz and the maximum ratio combining (MRC) technique is applied at the destination for the incoming signals from the source and the relay.

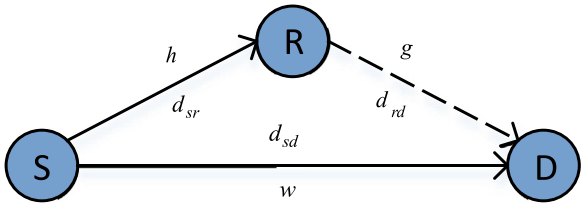

Fig. 1. Considered EH cooperative AF relay network.

- Simulation and theoretical results are obtained for different system parameters. By using a power constraint relay, the obtained diversity gains are evaluated.
- The impact of PS and TS factors on the BER performance of the considered system is investigated.
- For PS, TS and ideal modes, our results show that positioning the relay in the middle of the source and destination yields the optimum BER performance.
- The impact of energy conversion factor on the BER performance is evaluated. It is shown that higher the energy conversion factor, the better is the BER performance.

In this paper, it is assumed that all nodes are equipped by one antenna and all links are exposed to Nakagami-m fading. Non-EH direct and non-EH cooperative AF transmission networks are considered as reference schemes for comparison purposes.

1.3. Organization

The remainder of the paper is follows as: System model is given in Section 2. Unified BEP analysis is performed in Section 3. Section 4 deals with theoretical and computer simulation results and finally Section 5 concludes the paper.

2. System model

The considered cooperative relaying network consists of a source (S) communicating with a destination (D) over a direct link and an EH-AF relay (R) as shown in Fig. 1. The source and the destination have consistent power supplies while the relay harvests energy and processes information from the incoming signal from the source. PS, TS and ideal operational modes are considered at the relay for EH. The envelope of the channel fading coefficients of the links S→D, S→R and R→D are assumed as Nakagami-m distributed random variables, denoted by w, h and g with Nakagami-m parameters m_w, m_h and m_g, as well as $\Omega_w = E\left\{|w|^2\right\}$, $\Omega_h = E\left\{|h|^2\right\}$ and $\Omega_g = E\left\{|g|^2\right\}$, respectively. In our system model, it is assumed that the CSI is perfectly known at all receivers. Note that the BER performances will dramatically degrade when the CSI is not known at the receivers. s is the transmitted data symbol from the source where $E\left\{|s|^2\right\} = 1$. n_i, $i \in \{sd, sr, rd\}$ represent complex additive white Gaussian noise (AWGN) samples distributed as $\mathcal{N}(0, \sigma_i^2)$ per dimension where $2\sigma_i^2 = N_0$. Furthermore, d_{sd}, d_{sr} and d_{rd} stand for distances of the links S→D, S→R and R→D, respectively. In order to maintain the path-loss smaller than one for the distances smaller than unity, we adopt a bounded path-loss model as in [17]. Consequently, the path-loss is taken as $L_i = 1/(1 + d_i^{\xi})$, where $i \in \{sd, sr, rd\}$ and ξ is the path loss coefficient, which guarantees that L_i is always smaller than one. P_t, P_s and P_r are the total, source and relay transmit powers, respectively. As shown in Fig. 2, the overall transmission of T seconds concerns two signaling intervals. At the first interval, the transmitted signal from the source is received at the destination from the direct link, meanwhile, it is also received by the relay from which it harvests energy and processes the

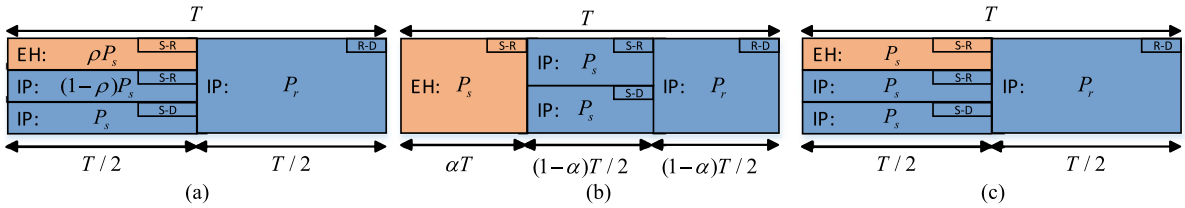

Fig. 2. Time schedule for (a) PS, (b) TS and (c) Ideal operational modes.

source information. Then, at the second signaling interval, the normalized received signal is amplified and forwarded to the destination by the relay using the total harvested energy. Finally, the destination applies MRC to the received signals to decode the source information. The received signals at the destination from the direct link and the relay are given by

$$y_{sd} = \sqrt{P_s L_{sd}} w s + n_{sd} \tag{1}$$

and

$$y_{rd} = \sqrt{(P_r L_{rd}/G)} y_{sr} g + n_{rd} \tag{2}$$

respectively, where G is the normalization power factor taking different values for the studied three different EH operational modes and y_{sr} is the received signal for information processing at the relay node. For EH at the relay, PS, TS and ideal operational modes are considered in the sequel.

2.0.1. PS EH-AF operational mode

For PS, the power proportion for the relay to harvest energy and to process the source signal is taken as ρ. At the first signaling interval of $T/2$ seconds, the received signal at the relay for IP is given by

$$y_{sr} = \sqrt{(1-\rho) P_s L_{sr}} h s + n_{sr}. \tag{3}$$

The harvested energy is calculated as $E_H = \eta\rho P_s L_{sr} |h|^2 (T/2)$ where $0 < \eta \leqslant 1$ is the energy conversion factor [2]. Considering the total power-constraint of P_t for the system and the energy constraint of $P_t T = P_s T/2$, we have $P_s = 2P_t$, $P_r = E_H/(T/2) = \eta\rho P_s L_{sr} |h|^2$ and $G = P_s |h|^2 (1-\rho) L_{sr} + \sigma_{sr}^2$. Substituting in (2), the received signal from link R→D, during the second interval of $T/2$ seconds, is written as

$$y_{rd} = \frac{\sqrt{\eta |h|^2 J L_{sr} L_{rd}}}{N} P_s h g s + \frac{\sqrt{\eta P_s |h|^2 \rho L_{rd}}}{N} g n_{sr} + n_{rd} \tag{4}$$

where $N = \sqrt{P_s |h|^2 (1-\rho) + \sigma_{sr}^2 / L_{sr}}$ and $J = \sqrt{\rho(1-\rho)}$.

2.0.2. TS EH-AF operational mode

For TS, the first and second signaling intervals are of durations $\alpha T + (1-\alpha T)/2$ and $(1-\alpha T)/2$ seconds, respectively. At the first signaling interval, αT and $(1-\alpha T)/2$ seconds are designated for EH and IP at the relay, respectively. The received signal for IP at the relay is given by $y_{sr} = \sqrt{P_s L_{sr}} h s + n_{sr}$. The harvested energy is calculated as $E_H = \eta P_s L_{sr} |h|^2 \alpha T$. At the second signaling interval, the received signal from link R→D is given by (2) where $P_r = 2E_H/(1-\alpha)T = \eta(2\alpha/(1-\alpha)) P_s L_{sr} |h|^2$ and $G = P_s |h|^2 L_{sr} + \sigma_{sr}^2$. Assuming that a total power of P_t is consumed in T seconds, the energy constraint for TS is given as $P_t T = P_s \alpha T + P_s (1-\alpha) T/2$, where after simplifying $P_s = 2P_t/(1+\alpha)$ is obtained. Substituting in (2), the received signal at the destination is given as

$$y_{rd} = \frac{\sqrt{J\eta |h|^2 L_{sr} L_{rd}}}{N} P_s h g s + \frac{\sqrt{J\eta P_s |h|^2 L_{rd}}}{N} g n_{sr} + n_{rd} \tag{5}$$

where $N = \sqrt{P_s |h|^2 + \sigma_{sr}^2 / L_{sr}}$ and $J = 2\alpha/(1-\alpha)$.

2.0.3. Ideal EH-AF operational mode

For the ideal operational mode, in the first signaling interval of $T/2$ seconds, the received signals at the destination and the relay are given as in (1) and $y_{sr} = \sqrt{P_s L_{sr}} h s + n_{sr}$, respectively. Furthermore, the amount of harvested energy is $E_H = \eta P_s L_{sr} |h|^2 (T/2)$. Considering the total power of PS case, we have $P_s = 2P_t$. In the next interval of $T/2$ seconds, the received signal at the relay is normalized, amplified and forwarded to the destination where it is received as in (2), with $G = P_s |h|^2 L_{sr} + \sigma_{sr}^2$ and $P_r = 2E_H/T = \eta P_s L_{sr} |h|^2$. Substituting in (2), the received signal at the destination is given as

$$y_{rd} = \frac{\sqrt{\eta |h|^2 L_{sr} L_{rd}}}{N} P_s h g s + \frac{\sqrt{\eta P_s |h|^2 L_{rd}}}{N} g n_{sr} + n_{rd} \tag{6}$$

where $N = \sqrt{P_s |h|^2 + \sigma_{sr}^2 / L_{sr}}$.

3. Bit error probability analysis

In this section, we provide a unified approach for the BEP calculation of the AF relaying-aided cooperative EH system. For the cooperative AF relaying system, the SNR at the destination node can be written as

$$Z = X + Y \tag{7}$$

where Z, X and Y stand for γ_{AF}, γ_{sd} and γ_{srd} for clarity of presentation, respectively. Here, $\gamma_{sd} = P_s L_{sd} |w|^2 / \sigma_{sd}^2$ is the SNR for the link S→D and it is calculated from (1) in which CDF of γ_{sd} is given in [18, 2.3-24] as

$$F_X(x) = 1 - \exp(-\frac{m_w}{F\Omega_w} x) \sum_{l=0}^{m_w - 1} \frac{1}{l!} (\frac{m_w}{F\Omega_w} x)^l \tag{8}$$

where $F = P_s L_{sd} / \sigma_{sd}^2$. Moreover, a unified SNR for the link S→R→D is calculated from the received signals in (4), (5) and (6) as

$$Y = \frac{A |h|^4 |g|^2}{B |h|^2 |g|^2 + C |h|^2 + D} \tag{9}$$

where the constants A, B, C and D are defined for each specific EH operational mode. For PS case, $A = \eta\rho P_s^2 (1-\rho)$, $B = \eta\rho P_s \sigma_{sr}^2 / L_{sr}$ and $C = (1-\rho) P_s \sigma_{rd}^2 / L_{sr} L_{rd}$. For TS case, $A = \eta 2\alpha P_s^2 / (1-\alpha)$, $B = \eta 2\alpha P_s \sigma_{sr}^2 / L_{sr} (1-\alpha)$ and $C = P_s \sigma_{rd}^2 / L_{sr} L_{rd}$. For the ideal case, $A = \eta P_s^2$, $B = \eta P_s \sigma_{sr}^2 / L_{sr}$ and $C = P_s \sigma_{rd}^2 / L_{sr} L_{rd}$. Finally, $D = \sigma_{sr}^2 \sigma_{rd}^2 / L_{sr} L_{rd}$ and it is the same for all operational modes. The CDF of Y at high SNR, where $D \simeq 0$, is calculated in [16] as

$$F_Y(y) = 1 - \varepsilon \exp(-\mu y) y^\beta K_\nu \left(2\delta \sqrt{y}\right). \tag{10}$$

where $K_\nu(\cdot)$ represents the νth-order modified Bessel function of the second kind [19, 8.407] and $\varepsilon = \frac{2}{\Gamma(m_g)} \sum_{k=0}^{m_h - 1} \sum_{i=0}^{k} T(k,i)$, $\mu = m_h B / \Omega_h A$, $\nu = m_g - i$, $\delta = \sqrt{m_h m_g C / \Omega_h \Omega_g A}$ and $\beta = (m_g - i + 2k)/2$. Here,

$$T(k,i) = \frac{1}{(k-i)!\, i!} \left(\frac{m_h}{\Omega_h A}\right)^\beta \left(\frac{C m_g}{\Omega_g}\right)^{\frac{m_g + i}{2}} B^{k-i}. \tag{11}$$

3.1. CDF calculation of Z

In this subsection, we evaluate the CDF of Z to obtain the SEP of the system. CDF of Z in (7) is expressed as [20, Chap. 6]

$$F_Z(z) = P(X + Y < z) = \int_{y=0}^{z} f_Y(y) F_X(z-y) dy. \tag{12}$$

where $f_Y(y)$ and $F_X(x)$ are the probability density function (PDF) of random variable (r.v.) Y and CDF of r.v X, respectively. Substituting $F_X(x)$ from (8) in (12), simplifying and using binomial expansion [19, 1.111], we have

$$F_Z(z) = F_Y(z) - \theta\phi \exp\left[z(-m_w/F\Omega_w)\right](-z)^{l-j} \times \int_{y=0}^{z} f_Y(y) \exp\left[(m_w/F\Omega_w)y\right] y^j dy \tag{13}$$

where $\theta = \sum_{l=0}^{m_w-1} \frac{1}{l!}(\frac{m_w}{F\Omega_w})^l$ and $\phi = (-1)^l \sum_{j=0}^{l} \binom{l}{j}$. Using the integration by parts, (13) can be expressed as

$$F_Z(z) = U_1 - U_2 + U_3 \tag{14}$$

where $U_1 = F_Y(z)$, $U_2 = \theta\phi(-1)^{l-j} z^l F_Y(z)$,

$$U_3 = \theta\phi(-1)^{l-j} e^{(-zm_w/F\Omega_w)} z^{l-j} \left[\frac{m_w}{F\Omega_w} R_1 + jR_2\right].$$

Here,

$$R_i = \int_{y=0}^{z} F_Y(y) e^{(ym_w/F\Omega_w)} y^\tau dy \tag{15}$$

where $i \in \{1, 2\}$ and $\tau = j$ and $j-1$ for $i = 1$ and 2, respectively. Substituting (10) in (15), we have

$$R_i = E_{i1} - E_{i2} \tag{16}$$

where

$$E_{i1} = \int_{y=0}^{z} e^{(ym_w/F\Omega_w)} y^\tau dy \tag{17}$$

and

$$E_{i2} = \varepsilon \int_{y=0}^{z} \exp(y(-\mu + \frac{m_w}{F\Omega_w})) y^{\beta+\tau} K_v\left(2\delta\sqrt{y}\right) dy. \tag{18}$$

Using [19, (2.33-10)] in (17), we obtain,

$$E_{i1} = \frac{\Gamma(\tau+1, 0)}{(-m_w/F\Omega_w)^{\tau+1}} - \frac{\Gamma(\tau+1, -zm_w/F\Omega_w)}{(-m_w/F\Omega_w)^{\tau+1}}. \tag{19}$$

where $\Gamma(\cdot,\cdot)$ is the incomplete gamma function [19, 8.350]. In order to solve the integral in (18), we use the series expansion of $\exp(\cdot)$ function [19, (1.211-1)] and express $K_v(\cdot)$ as a Meijer's G function [21, (14)]; which yields

$$E_{i2} = \frac{\varepsilon}{2} \sum_{p=0}^{\infty} \frac{1}{p!}(-\mu + \frac{m_w}{F\Omega_w})^p \times \int_{y=0}^{z} y^{p+\beta+\tau} G_{0,2}^{2,0}\left(\delta^2 y \middle|_{v/2,-v/2}^{-}\right) dy. \tag{20}$$

Using [22, (4.264)], (20) can be rewritten as

$$E_{i2} = \frac{\varepsilon}{2} \sum_{p=0}^{\infty} \frac{1}{p!}(-\mu + \frac{m_w}{F\Omega_w})^p z^{p+\beta+\tau+1} \times G_{1,3}^{2,1}\left(\delta^2 z \middle|_{v/2,-v/2,-(p+\beta+\tau+1)}^{1-(p+\beta+\tau+1)}\right). \tag{21}$$

Finally, substituting (19), (21) for $i = 1$ and 2 in (16), and then (16) in (14), the CDF of Z in (7) is obtained as follows

$$F_Z(z) = F_Y(z) - \sum_{l=0}^{m_w-1} \frac{1}{l!}(\frac{m_w}{F\Omega_w})^l (-1)^l \sum_{j=0}^{l} \binom{l}{j} (-1)^{l-j} \times \left(z^l F_Y(z) + e^{(-zm_w/F\Omega_w)} z^{l-j} \left[\left(\frac{m_w}{F\Omega_w} E_{11} + jE_{21}\right) - \left(\frac{m_w}{F\Omega_w} E_{12} + jE_{22}\right)\right]\right). \tag{22}$$

3.2. BEP calculation

The SEP for the cooperative AF relaying system can be given from [23] as

$$P_{SER} = \frac{a\sqrt{b}}{2\sqrt{\pi}} \int_0^\infty \frac{e^{-bz}}{\sqrt{z}} F_Z(z) dz = \frac{a\sqrt{b}}{2\sqrt{\pi}} \left[V_1 - \sum_{l=0}^{m_w-1} \frac{1}{l!}(\frac{m_w}{F\Omega_w})^l (-1)^l \times \sum_{j=0}^{l} \binom{l}{j} (-1)^{l-j} (V_2 + W_1 - W_2)\right] \tag{23}$$

where a and b are modulation specific constants [23, (35)]. Here, $F_Z(z)$ is given in (22) and V_1, V_2, W_1 and W_2 are given as

$$V_i = \int_0^\infty \frac{e^{-bz}}{\sqrt{z}} z^\omega F_Y(z) dz \tag{24}$$

where $i \in \{1, 2\}$ and $\omega = 0$ and l for $i = 1$ and 2, respectively, and

$$W_i = \int_0^\infty \frac{e^{-bz}}{\sqrt{z}} e^{(-zm_w/F\Omega_w)} z^{l-j} \left(\frac{m_w}{F\Omega_w} E_{1i} + jE_{2i}\right) dz \tag{25}$$

for $i \in \{1, 2\}$.

3.2.1. Calculation of V_1 and V_2

Using (24) we obtain,

$$V_i = \int_0^\infty \frac{e^{-bz}}{\sqrt{z}} z^\omega F_y(z) dz = V_{i1} - \varepsilon V_{i2}. \tag{26}$$

In (26), using [19, (3.381)],

$$V_{i1} = \int_0^\infty \frac{e^{-bz}}{\sqrt{z}} z^\omega dz = \frac{1}{b^{(\omega+0.5)}} \Gamma(\omega + 0.5) \tag{27}$$

and

$$V_{i2} = \int_0^\infty \frac{e^{-bz}}{\sqrt{z}} z^\omega \exp(-\mu y) y^\beta K_v\left(2\delta\sqrt{y}\right) dz. \tag{28}$$

Considering the integral variable $z = \xi^2$, $\Theta = \mu + b$, $\varpi = \beta - 0.5 + \omega$, $\Upsilon = 2\delta$ and using [19, (6.631-3)] we have

$$V_{i2} = \Theta^{-0.5\Delta} \Upsilon^{-1} \Gamma\left(\frac{1+\nu+\Delta}{2}\right) \Gamma\left(\frac{1-\nu+\Delta}{2}\right) \times \exp\left(\frac{\Upsilon^2}{8\Theta}\right) W_{-0.5\Delta, 0.5\nu}\left(\frac{\Upsilon^2}{4\Theta}\right) \tag{29}$$

where $\Delta = 2\varpi + 1$, $\Gamma(\cdot)$ and $W_{\cdot,\cdot}(\cdot)$ are the gamma and Whittaker functions given in [19, 8.310] and [19, 9.220], respectively. Moreover, ν and β are defined in [16]. Finally, substituting (27) and (29) for $i = 1$ and 2 in (26), we obtain V_1 and V_2 and then substitute them in (23).

3.2.2. Calculation of W_1

From (25), W_1 can be expressed as

$$W_1 = \frac{m_w}{F\Omega_w} Q_1 + jQ_2 \tag{30}$$

where

$$Q_i = \int_0^\infty \frac{e^{-bz}}{\sqrt{z}} e^{(-zm_w/F\Omega_w)} z^{l-j} E_{i1} dz \tag{31}$$

for $i \in \{1, 2\}$. Substituting (19) for $i = 1$ and 2 in (31), simplifying and using [19, (3.381-4)] and [19, (6.445-1)], we obtain

$$\begin{aligned} Q_i = {} & \frac{\Gamma(\kappa+1)}{(-m_w/F\Omega_w)^{\kappa+1}} (b + \frac{m_w}{F\Omega_w})^{-(l-j+0.5)} \\ & \times \Gamma(l-j+0.5) - \frac{\Gamma(l-j+1.5+\kappa)}{(l-j+0.5) b^{l-j+1.5+\kappa}} \\ & \times {}_2F_1\left(1, l-j+1.5+\kappa; l-j+1.5; \frac{b+\frac{m_w}{F\Omega_w}}{b}\right) \end{aligned} \tag{32}$$

where for $i = 1$ and 2, we replace $\kappa = j$ and $\kappa = j-1$, respectively.

3.2.3. Calculation of W_2

From (25), W_2 can be written as

$$W_2 = \frac{m_w}{F\Omega_w} N_1 + jN_2 \tag{33}$$

where

$$N_i = \int_0^\infty \frac{e^{-bz}}{\sqrt{z}} e^{(-zm_w/F\Omega_w)} z^{l-j} E_{i2} dz \tag{34}$$

for $i \in \{1, 2\}$. Substituting (21) for $i = 1$ and 2 in (34), we obtain

$$\begin{aligned} N_i = {} & \frac{\varepsilon}{2} \sum_{p=0}^{\infty} \frac{1}{p!} (-\mu + \frac{m_w}{F\Omega_w})^p \int_0^\infty e^{(-z(b+m_w/F\Omega_w))} \\ & \times z^{l-j+p+\beta+\zeta+0.5} G_{1,3}^{2,1}\left(\delta^2 z \middle| \begin{matrix} 1-(p+\beta+\zeta+1) \\ v/2, -v/2, -(p+\beta+\zeta+1) \end{matrix}\right) dz. \end{aligned} \tag{35}$$

where $i \in \{1, 2\}$ and $\zeta = j$ and $j-1$ for $i = 1$ and 2, respectively. In order to calculate the integral in (35), we express exp(·) function as a Meijer'G function [22, (4.264)] and using [19, (9.31-1)], (35) can be rewritten as

$$\begin{aligned} N_i = {} & \frac{\varepsilon}{2} \sum_{p=0}^{\infty} \frac{1}{p!} (-\mu + \frac{m_w}{F\Omega_w})^p \\ & \times \int_0^\infty z^{l-j+p+\beta+\zeta+0.5} G_{1,2}^{1,1}\left(z(b + \frac{m_w}{F\Omega_w}) \middle|_{0,0}^{0}\right) \\ & \times G_{1,3}^{2,1}\left(\delta^2 z \middle| \begin{matrix} 1-(p+\beta+\zeta+1) \\ \frac{v}{2}, -\frac{v}{2}, -(p+\beta+\zeta+1) \end{matrix}\right) dz. \end{aligned} \tag{36}$$

Using [21, (21)], (36) can be obtained as:

$$\begin{aligned} N_i = {} & \frac{\varepsilon}{2} \sum_{p=0}^{\infty} \frac{1}{p!} (-\mu + \frac{m_w}{F\Omega_w})^p (b + m_w/F\Omega_w)^{-\varrho_i} \\ & \times G_{3,4}^{3,2}\left(\frac{\delta^2}{(b+m_w/F\Omega_w)} \middle| \begin{matrix} 1-(p+\beta+\zeta+1), 1-\varrho_i, 1-\varrho_i \\ \frac{v}{2}, -\frac{v}{2}, 1-\varrho_i, -(p+\beta+\zeta+1) \end{matrix}\right) \end{aligned} \tag{37}$$

where $\varrho_i = l-j+p+\beta+\zeta+1.5$. Substituting $\zeta = j$ and $j-1$ for $i = 1$ and 2 in (37) and then in (33), respectively, W_2 is obtained.

Finally, substituting (24) for $i = 1$ and 2, (30) and (33) in (23), SEP can be calculated. Using the common approximation [24] at high SNR, BEP can be expressed as

$$P_{BER} \simeq P_{SER}/k \tag{38}$$

where $k = \log_2 M$, M being the modulation order.

4. Performance evaluation

In this section, we verify the derived closed-form end-to-end BEP expressions through Monte Carlo simulations for EH cooperative AF relaying system in the Nakagami-m fading channel. Considering the obtained results, we get insights into the impact of the considered system parameters on the BER performance. A co-linearly located three-node (source–relay–destination) network is considered and the source to destination distance is normalized and fixed to unity while the relay location is arbitrary. Unless otherwise specified, we set $\eta = 1$ as in [3], $d_{sr} = 0.5$ and SNR = 20 dB. The noise samples at the relay and destination nodes are assumed to have equal variance as $\sigma^2 = \sigma_{sr}^2 = \sigma_{sd}^2 = \sigma_{rd}^2$ and $\Omega_w = \Omega_h = \Omega_g = 1$. Moreover, we set the path-loss exponent to $\xi = 2.7$ as in [25], which is valid in urban cellular network environment. In all figures, theoretical and computer simulation results are denoted by straight lines and markers, respectively. The theoretical BEP of the EH cooperative AF system is obtained by replacing (23) in (38). DH-EH [16] and non-EH cooperative AF [26] transmission systems are considered for the comparison purposes. In Figs. 3–6, [1 1 1], [1 2 2] and [2 2 2] stand for the Nakagami-m channel parameters [m_w m_h m_g]. Also, [1 1] and [2 2] represents [m_h m_g] for the DH-EH system [16]. System performance results are obtained for the spectral efficiency of $R = 1$ bit/s/Hz for which to have a fair comparison between the proposed and reference systems, the source power (P_s) is calculated considering the total energy constraint ($E_h = P_t T$) of the system in time interval T, as $2P_t/(1+\alpha)$, $2P_t$ and $2P_t$ for TS, PS and ideal transmission systems, respectively. Meanwhile, source and relay powers of the non-EH cooperative AF [26] scheme are both set to P_t. Moreover, for $R = 1$ bit/s/Hz, PS, ideal and non-EH cooperative AF systems transmission apply 4-QAM. Besides, for the TS operational mode, we consider the mixture of modulations given in [16, Table I] to maintain the spectral efficiency fixed at $R = 1$ bit/s/Hz.

For PS and ideal EH operational modes, BER should be computed over the total IP time interval, which is equal to T. However, this time interval is equal to $(1-\alpha)T$ for TS. Therefore, to evaluate the obtained results on an equal spectral efficiency basis, we adopted the idea of mixture of modulations for TS, previously given in [14] and generalized for different spectral efficiency values in [16]. In TS, as α increases, EH time interval increases against IP time interval, which itself decreases. As a result, by increasing the value of α, we have to increase the modulation order to ensure the same total number of transmitted bits and to maintain the spectral efficiency of the considered three EH operational modes at the same value.

In Fig. 3, BER curves are depicted versus SNR where for each SNR value, the corresponding numerically obtained optimum ρ and α values, which minimize the system BER performance, are considered, for PS and TS, respectively. It is observed from this figure that the simulation and theoretical curves are in perfect match. From Fig. 3(a), at a BER value of 10^{-3}, we approximately have 9, 8 and 8 dB SNR gains for PS, TS and ideal operational modes for channel parameters [1 2 2], respectively, compared to the DH-EH with [2 2]. Moreover, diversity gains of 1.83, 1.73 and 1.82 are obtained for the PS, TS and ideal operational modes when the channel parameters are [1 1 1], while these values are 2.54, 2.36 and 2.57 for [1 2 2], respectively. On the other hand, from Fig. 3(b), at a BER value of 10^{-2}, SNR gains of 13, 14 and 13 dB for PS, TS and ideal cases are provided, respectively,

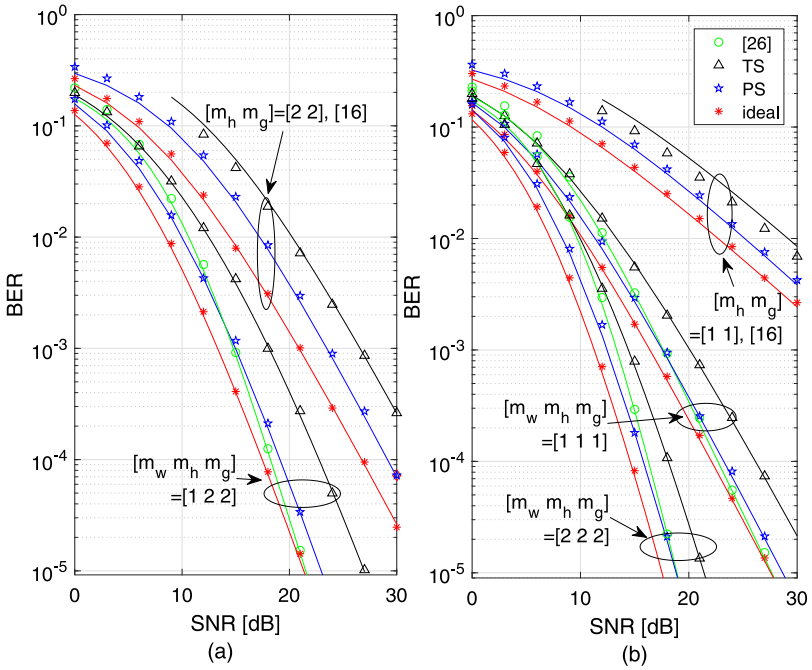

Fig. 3. BER performance versus SNR for channel parameters (a) [2 2] and [1 2 2], (b) [1 1], [1 1 1] and [2 2 2].

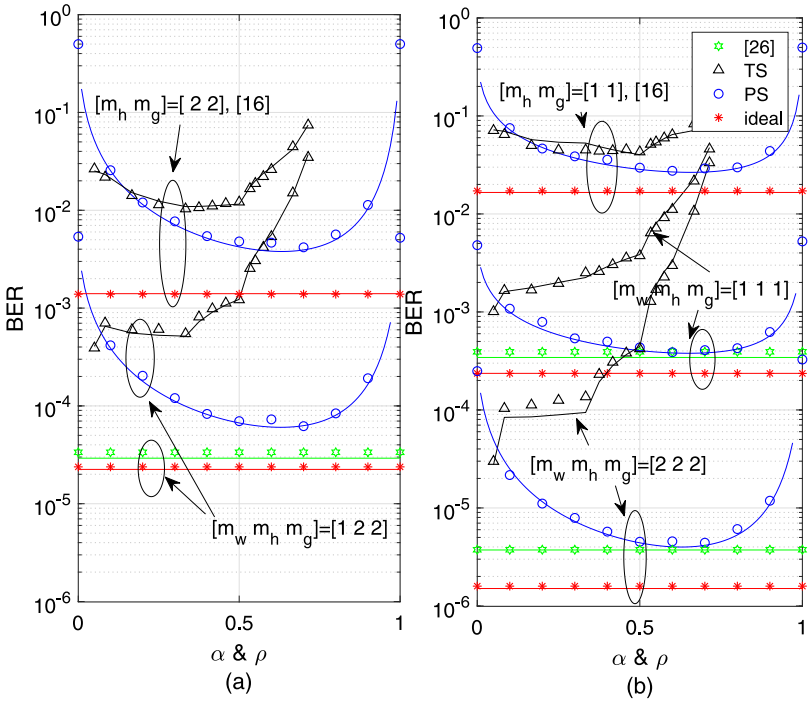

Fig. 4. BER performance versus ρ and α for channel parameters (a) [2 2] and [1 2 2], (b) [1 1], [1 1 1] and [2 2 2].

compared to the DH-EH with [1 1], for channel parameters [1 1 1]. Also, diversity gains are 3.11, 3 and 3.38 for PS, TS and ideal operational modes, for channel parameters [2 2 2], respectively. Moreover, from Fig. 3(a), at a BER value of 10^{-4}, the non-EH cooperative AF system outperforms PS operational mode for the channel parameters [1 1 1] and [1 2 2] at the SNR values higher than 18 and 12 dB, respectively. However, from Fig. 3(b), for the case [2 2 2], PS operational mode becomes better than the non-EH cooperative AF system. This is due to the fact that for PS mode, the total energy of P_tT is consumed at the source during $T/2$ seconds, and the source power is equal to $2P_t$. However, for the non-EH cooperative AF scheme the total energy P_tT are equally divided to the source and the relay, which both having a power of P_t. As a result, S→D link is improved with respect to the non-EH case, moreover, the relay provides additional diversity by its harvested energy. Note that at a BER value of 10^{-4}, we have 3, 5 and 2 dB SNR penalties against TS in comparison to non-EH cooperative AF for channel parameter values [1 1 1], [1 2 2] and [2 2 2], respectively.

In Fig. 4, BER performance curves are plotted against PS and TS parameters, ρ and α, respectively. It can be seen from this figure that the theoretical curves obtained from the closed-form

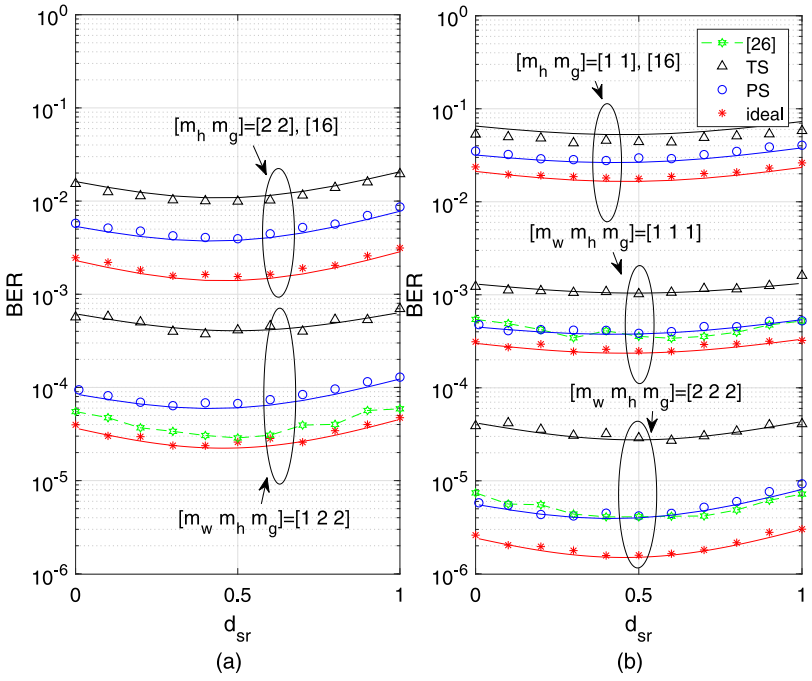

Fig. 5. BER performance versus S→R distance for channel parameters (a) [2 2] and [1 2 2], (b) [1 1], [1 1 1] and [2 2 2], $d_{sr} + d_{rd} = 1$.

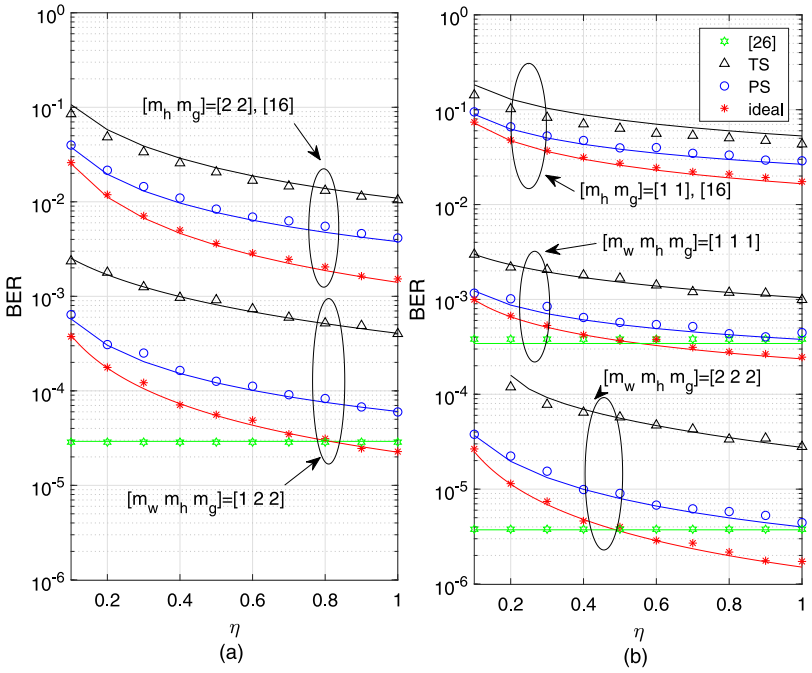

Fig. 6. BER performance versus energy conversion factor η for channel parameters (a) [2 2] and [1 2 2], (b) [1 1], [1 1 1] and [2 2 2].

BEP expression derived above are very close to the computer simulation curves. It is observed from Fig. 4 that for TS mode with channel parameter values [1 1 1], [1 2 2] and [2 2 2], the BER is minimized for the smallest value of α for which 4-QAM is employed as in [16, Table I]. On the other hand, for PS, the optimum ρ values minimizing the BER are 0.65, 0.63 and 0.63 for channel parameters [1 1 1], [1 2 2] and [2 2 2], respectively. It is also observed from Fig. 4 that for ρ or α values smaller than 0.07, TS performance is better than PS. From Fig. 4(a) and (b), the BER performances of PS, TS and ideal operational modes are improved by 98.41%, 96.27% and 98.40% compared to the DH-EH with [2 2] for [1 2 2] and by 98.57%, 97.68% and 98.57%, compared to the DH-EH with [1 1] for [1 1 1], respectively. Moreover, it is seen from Fig. 4(a) and (b) that non-EH cooperative AF outperforms TS mode for the considered three channel parameter settings. However, PS and non-EH cooperative AF have the same BER performance for [1 1 1] and [2 2 2] except [1 2 2] for which non-EH cooperative AF outperforms PS mode.

Remark 1. Unlike the optimum value of α, which is equal to 1/3 for TS mode in [16] where no direct link is available between source and destination, for the studied EH cooperative AF system, the minimum α value is optimum in terms of BER performance, which is due to the presence of direct link. In other words, since

there is a direct link between the source and destination, for TS mode, less time (less α) is needed for the relay to harvest energy. Finally, please note that since specific α values are considered to apply the mixture of modulations, the obtained curves in Fig. 4 are not smooth for TS case.

BER performance is evaluated against the source-to-relay distance (d_{sr}) in Fig. 5, for different channel parameters. In Fig. 5, for each value of d_{sr}, the numerically obtained optimum ρ and α values minimizing the BER for PS and TS operational modes are considered. From Fig. 5(a) and (b), it is seen that the optimum d_{sr} value minimizing the BER is nearly 0.47 for all EH operational modes. Note also that the BER performance is highly affected by the channel parameters. PS and non-EH cooperative AF system have approximately the same performance for [1 1 1] and [2 2 2] while for [1 2 2] there is a BER penalty against PS compared to the non-EH cooperative AF system. Meanwhile, non-EH cooperative AF outperforms TS operational mode for all channel parameter settings.

Fig. 6 plots the BER performance of the considered EH cooperative AF system versus energy conversion factor η. As done for the previous system parameters, for each value of η, optimum ρ and α values minimizing the BER are numerically obtained and considered in Fig. 6(a) and (b), for PS and TS modes, respectively. Moreover, from Fig. 6(a) and (b) the BER performances of PS, TS and ideal operational modes are improved by 98.41%, 96.27% and 98.40% compared to DH-EH with [2 2] for [1 2 2] and by 98.57%, 98.03% and 98.6%, compared to DH-EH with [1, 1] for [1 1 1], respectively. It is observed that the ideal operating mode outperforms non-EH cooperative AF for η values larger than 0.5, 0.8 and 0.5 for [1 1 1], [1 2 2] and [2 2 2], respectively. Furthermore, for $\eta = 1$, PS mode provides the same BER performance as non-EH cooperative AF system for [1 1 1] and [2 2 2] while non-EH cooperative AF outperforms PS mode even when $\eta = 1$ for [1 2 2]. Finally, TS mode has a worse BER performance compared to PS, ideal and non-EH cooperative AF for all values of η.

Remark 2. We finally analyze the power budget of the relay power based on the source power. Note that for PS, TS, ideal and non-EH cooperative AF systems relay powers are $P_r = \eta\ \rho\ Ps\ L_{sr}\ |h|^2$, $P_r = \eta\ 2\alpha\ Ps\ L_{sr}\ |h|^2/(1-\alpha)$, $P_r = \eta\ Ps\ L_{sr}\ |h|^2$ and $P_r = P_s$, respectively. On the other hand, for PS, TS, ideal and non-EH cooperative AF systems, $P_s = 2P_t$, $P_s = 2P_t/(1+\alpha)$, $P_s = 2P_t$ and $P_s = P_t$, respectively. Fig. 7 plots the harvested power P_r versus P_s. For the PS and TS cases, we assume $\rho = 0.8$ and $\alpha = 1/20$ (obtained from [16, Table I]), respectively. Curves for P_r are provided for $d_{sr} = 0.5$ and $d_{sr} = 1$. It can be seen from Fig. 7 that the path loss has a crucial effect on the amount of harvested power P_r. For example, for the TS case and for $P_s = 10.8$ dB, we have $P_r = 0.3997$ dB and $P_r = -1.998$ dB for $d_{sr} = 0.5$ and $d_{sr} = 1$, respectively. The same trend can be followed for the PS and ideal cases while for the non-EH cooperative AF system $P_r = P_s$.

Remark 3. Since the obtained theoretical and simulation curves in Figs. 3–6 match considerably well with each other, the tightness of the BER expression given in (38) is verified.

Remark 4. A cooperative selective DF relaying system where the relay is an EH node, is considered in [27]. This system has comparable results to the cooperative AF system. However, cooperative DF EH (non-selective) is not considered since it has a worse BER performance compared to the two other systems mentioned above due to the error propagation. In fact, in non selective DF relaying system, the relay always forwards the signals to the destination without taking into account the correct detection of the signal, which results in error propagation at the destination.

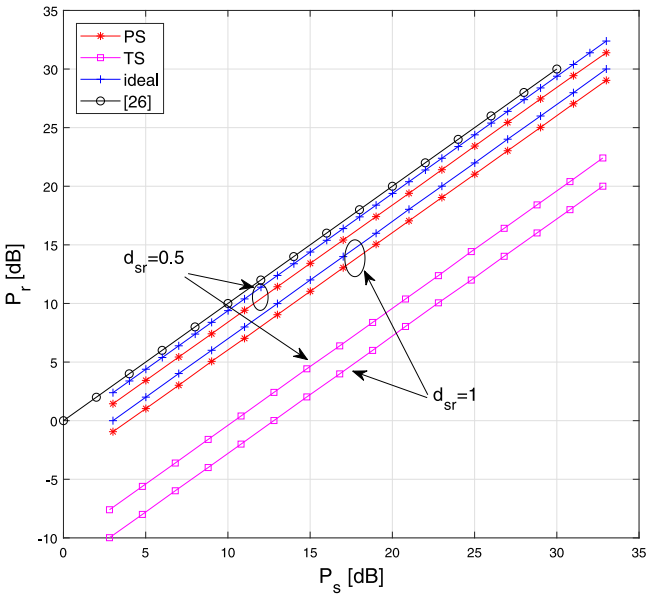

Fig. 7. Power budget of the relay versus source power.

5. Conclusion

In this paper, we have studied the bit error performance of the EH cooperative AF relaying system. We have provided a unified approach to the BEP analysis for PS, TS and ideal operational modes. A closed-form BEP expression has been obtained when all links are exposed to Nakagami-m fading. The results have been provided for various system parameters that give a comprehensive insight into the system performance. Besides, computer simulation results have been obtained in perfect match with theoretical results, which validate our derivations. We have shown that the PS mode outperforms the TS mode when EH parameters ρ and α are optimized with respect to the considered system parameters on SNR, the relay position and energy conversion factor.

References

[1] P. Grover, A. Sahai, Shannon meets Tesla: Wireless information and power transfer, in: Proc. 2010 IEEE Int. Symp. on Info. Theo., 2010, pp. 2363–2367, http://dx.doi.org/10.1109/ISIT.2010.5513714.
[2] X. Zhou, R. Zhang, C.K. Ho, Wireless information and power transfer: Architecture design and rate-energy tradeoff, IEEE Trans. Commun. 61 (11) (2013) 4754–4767, http://dx.doi.org/10.1109/TCOMM.2013.13.120855.
[3] A.A. Nasir, X. Zhou, S. Durrani, R.A. Kennedy, Relaying protocols for wireless energy harvesting and information processing, IEEE Trans. Wirel. Commun. 12 (7) (2013) 3622–3636, http://dx.doi.org/10.1109/TWC.2013.062413.122042.
[4] K.M. Rabie, B. Adebisi, M.S. Alouini, Wireless power transfer in cooperative DF relaying networks with log-normal fading, in: Proc. 2016 IEEE Global Commun. Conf. (GLOBECOM), 2016, pp. 1–6, http://dx.doi.org/10.1109/GLOCOM.2016.7842388.
[5] A.A. Nasir, X. Zhou, S. Durrani, R.A. Kennedy, Throughput and ergodic capacity of wireless energy harvesting based DF relaying network, in: Proc. 2014 IEEE Int. Conf. Commun. (ICC), 2014, pp. 4066–4071, http://dx.doi.org/10.1109/ICC.2014.6883957.
[6] Y. Gu, S. Aïssa, RF-Based energy harvesting in decode-and-forward relaying systems: Ergodic and outage capacities, IEEE Trans. Wirel. Commun. 14 (11) (2015) 6425–6434, http://dx.doi.org/10.1109/TWC.2015.2453418.
[7] N.P. Le, N.S. Vo, M.T. Hoang, Throughput analysis of energy harvesting MIMO relay systems over Nakagami-m fading channels, in: Proc. 2017 Int. Conf. on Recent Advances in Signal Process., in: Telecommun. Comput. (SigTelCom), 2017, pp. 164–169, http://dx.doi.org/10.1109/SIGTELCOM.2017.7849816.
[8] R. Tao, A. Salem, K.A. Hamdi, Adaptive relaying protocol for wireless power transfer and information processing, IEEE Commun. Lett. 20 (10) (2016) 2027–2030, http://dx.doi.org/10.1109/LCOMM.2016.2593877.

[9] C. Zhang, H. Du, J. Ge, Energy-efficient power allocation in energy harvesting two-way AF relay systems, IEEE Access 5 (2017) 3640–3645, http://dx.doi.org/10.1109/ACCESS.2017.2670641.
[10] Y. Liu, L. Wang, M. Elkashlan, T.Q. Duong, A. Nallanathan, Two-way relaying networks with wireless power transfer: Policies design and throughput analysis, in: Proc. 2014 IEEE Global Commun. Conf, 2014, pp. 4030–4035, http://dx.doi.org/10.1109/GLOCOM.2014.7037438.
[11] D.D. Tran, H.V. Tran, D.B. Ha, H. Tran, G. Kaddoum, Performance analysis of two-way relaying system with RF-EH and multiple antennas, in: Proc. 2016 IEEE 84th Veh. Technol. Conf. (VTC-Fall), 2016, pp. 1–5, http://dx.doi.org/10.1109/VTCFall.2016.7881156.
[12] Z. Mheich, V. Savin, Cooperative communication protocols with energy harvesting relays, in: Proc. 2017 Wireless Days, 2017, pp. 60–65, http://dx.doi.org/10.1109/WD.2017.7918116.
[13] Z. Zhou, M. Peng, Z. Zhao, Y. Li, Joint power splitting and antenna selection in energy harvesting relay channels, IEEE Signal Process. Lett. 22 (7) (2015) 823–827, http://dx.doi.org/10.1109/LSP.2014.2369748.
[14] C. Huang, P. Sadeghi, A.A. Nasir, BER Performance analysis and optimization for energy harvesting two-way relay networks, in: Proc. 2016 Australian Commun. Theo. Workshop (AusCTW), 2016, pp. 65–70, http://dx.doi.org/10.1109/AusCTW.2016.7433611.
[15] P. Liu, S. Gazor, I.M. Kim, D.I. Kim, Energy harvesting noncoherent cooperative communications, IEEE Trans. Wirel. Commun. 14 (12) (2015) 6722–6737, http://dx.doi.org/10.1109/TWC.2015.2458969.
[16] M. Babaei, U. Aygölü, E. Basar, BER Analysis of dual-hop relaying with energy harvesting in Nakagami-*m* fading channel, IEEE Trans. Wirel. Commun. 17 (7) (2018) 4352–4361, http://dx.doi.org/10.1109/TWC.2018.2823711.
[17] Z. Ding, I. Krikidis, B. Sharif, H.V. Poor, Wireless information and power transfer in cooperative networks with spatially random relays, IEEE Trans. Wirel. Commun. 13 (8) (2014) 4440–4453, http://dx.doi.org/10.1109/TWC.2014.2314114.
[18] J.G. Proakis, Digital Communications, McGraw-Hill, 1995.
[19] A. Jeffrey, D. Zwillinger, Table of Integrals, Series, and Products, Academic press, 2007.
[20] A. Papoulis, S. Pillai, Probability, Random Variables, and Stochastic Processes, McGraw-Hill, 2002.
[21] V.S. Adamchik, O.I. Marichev, The algorithm for calculating integrals of hypergeometric type functions and its realization in reduce system, in: Proc. of the Int. Symp. on Symbolic and Algebraic Comput., in: ISSAC '90, 1990, pp. 212–224, http://dx.doi.org/10.1145/96877.96930.
[22] P. Shankar, Fading and Shadowing in Wireless Systems, Springer, 2011.
[23] R.H.Y. Louie, Y. Li, B. Vucetic, Practical physical layer network coding for two-way relay channels: performance analysis and comparison, IEEE Trans. Wirel. Commun. 9 (2) (2010) 764–777, http://dx.doi.org/10.1109/TWC.2010.02.090314.
[24] M. Simon, M. Alouini, Digital Communication over Fading Channels, Wiley, 2005.
[25] H. Meyr, M. Moeneclaey, S. Fechtel, Digital Communication Receivers: Synchronization, Channel Estimation, and Signal Processing, John Wiley & Sons, Inc., New York, NY, USA, 1997.
[26] H. Li, Q. Zhao, Distributed modulation for cooperative wireless communications, IEEE Signal Process. Mag. 23 (5) (2006) 30–36, http://dx.doi.org/10.1109/MSP.2006.1708410.
[27] M. Babaei, Ü. Aygölü, L. Durak-Ata, Performance of selective decode-and-forward SWIPT network in Nakagami-*m* fading channel, in: Proc. 2018 26th Telecommunications Forum (TELFOR), 2018, pp. 1–4, http://dx.doi.org/10.1109/TELFOR.2018.8612003.

Mohammadreza Babaei received his B.S. degree from Tabriz University, Tabriz, Iran, in 2011, and M.S. degree from Istanbul Technical University, Istanbul, Turkey, in 2016. He is currently a Ph.D. student and a member of Wireless communication laboratory in Istanbul Technical University, Istanbul, Turkey. He has served as a TPC member for several IEEE conferences and as a reviewer for IEEE journals. His research interests include MIMO systems, cognitive radio, cooperative communications, spatial modulation, energy harvesting and NOMA.

Umit Aygolu received his B.S., M.S. and Ph.D. degrees, all in electrical engineering, from Istanbul Technical University, Istanbul, Turkey, in 1978, 1984 and 1989, respectively. He was a Research Assistant from 1980 to 1986 and a Lecturer from 1986 to 1989, at Yildiz Technical University, Istanbul, Turkey. In 1989, he became an Assistant Professor at Istanbul Technical University where he became an Associate Professor and Professor in 1992 and 1999, respectively. His current research interests include MIMO systems, cooperative communications, cognitive radio, spatial modulation, energy harvesting and NOMA.

Ertugrul Basar received the B.S. degree (Hons.) from Istanbul University, Turkey, in 2007, and the M.S. and Ph.D. degrees from Istanbul Technical University, Turkey, in 2009 and 2013, respectively. He is currently an Associate Professor with the Department of Electrical and Electronics Engineering, Koç University, Istanbul, Turkey and the director of Communications Research and Innovation Laboratory (CoreLab). His primary research interests include MIMO systems, index modulation, waveform design, visible light communications, and signal processing for communications.

Recent recognition of his research includes the Science Academy (Turkey) Young Scientists (BAGEP) Award in 2018, Mustafa Parlar Foundation Research Encouragement Award in 2018, Turkish Academy of Sciences Outstanding Young Scientist (TUBA-GEBIP) Award in 2017, and the first-ever IEEE Turkey Research Encouragement Award in 2017.

Dr. Basar currently serves as an Editor of the IEEE Transactions on Communications and *Physical Communication* (Elsevier), and as an Associate Editor of the IEEE Communications Letters. He served as an Associate Editor for the IEEE Access from 2016 to 2018.